Magnetism and Hund's Rule in an Optical Lattice with Cold Fermions

K. Kärkkäinen,[1] M. Borgh,[1] M. Manninen,[2] & S.M. Reimann[1]

[1]*Mathematical Physics, LTH, Lund University, SE-22100 Lund, Sweden*
[2]*NanoScience Center, Department of Physics, FIN-40351 University of Jyväskylä, Finland*

Artificially confined, small quantum systems show a high potential for employing quantum physics in technology. Ultra-cold atom gases have opened an exciting laboratory in which to explore many-particle systems that are not accessible in conventional atomic or solid state physics[1]. It appears promising that optical trapping of cold bosonic or fermionic atoms will make construction of devices with unprecedented precision possible in the future, thereby allowing experimenters to make their samples much more "clean", and hence more coherent. Trapped atomic quantum gases may thus provide an interesting alternative to the quantum dot nanostructures[2] produced today. Optical lattices created by standing laser waves loaded with ultra-cold atoms are an example[1,3] of this. They provide a unique experimental setup to study *artificial crystal structures* with tunable physical parameters. Here we demonstrate that a two-dimensional optical lattice loaded with repulsive, contact-interacting fermions shows a rich and systematic magnetic phase diagram. Trapping a few ($N \leq 12$) fermions in each of the single-site minima of the optical lattice, we find that the *shell structure* in these quantum wells determines the magnetism. In a shallow lattice, the tunneling between the lattice sites is strong, and the lattice is non-magnetic. For deeper lattices, however, the shell-filling of the single wells with fermionic atoms determines the magnetism. As a consequence of Hund's first rule, the interaction energy is lowered by maximizing the number of atoms of the same species. This leads to a systematic sequence of non-magnetic, ferromagnetic and antiferromagnetic phases.

An optical lattice resembles an "egg box"-like arrangement of single quantum wells, each confining a small number of atoms. Different lattice geometries can be realized (see D. Jaksch and P. Zoller[3] for a review). The tunneling and the localization of atoms in the lattice are controlled by the lattice depth which can be tuned by changing the laser intensity. This allows for a smooth transition from a tightly bound lattice to a system of nearly free atoms. The confined atoms have many internal (hyperfine) states which can be manipulated by laser light. In a weakly interacting, dilute atom gas, s-wave scattering dominates. The strength of the short-ranged contact interaction between the atoms can be tuned in the vicinity of a Feshbach resonance[4,5,6,7,8,9].

For bosons in an optical lattice, it was possible to realize the Mott insulator-superfluid quantum phase transition[10,11,12,13]. More recently, a fermionic many-particle quantum system on a three-dimensional lattice was experimentally studied by Köhl *et al.*[14,15], who investigated the transition from a band insulator to a normal state.

The atom dynamics in an optical lattice is often described by the Hubbard or the Bose-Hubbard models[16] with the hopping parameter t and the on-site interaction parameter U. These models rely on the single-band approximation which allows at most two atoms in a lattice site in the fermionic case. From an experimental viewpoint, it has been argued that these discrete models are ideal for describing contact-interacting atoms in an optical lattice[10]. In condensed matter physics, the Hubbard model is constantly used to describe magnetic correlations in solids. In a deep lattice (with small t/U) for a half-filled band, or one fermion per site, the Hubbard model predicts antiferromagnetism. In fact, it can be shown that in this case the Hubbard Hamiltonian coincides with the antiferromagnetic Heisenberg model of localized atoms[17]. When the band is filled, each lattice site carries two fermions with opposite spins, and magnetism can not be observed. More recently, a SU(n) Hubbard model was applied to describe fermionic atoms with n different "flavors" or spin states[18].

Here, we go *beyond* the lowest-band approximation, applying the mean-field approach for a *two-component* system: We consider fermionic atoms with two hyperfine, or spin, species confined into a two-dimensional (square) lattice, where it is possible to trap a few ($N \leq 12$) atoms in each single well (at each single site). We find that depending on the statistics and the spin of the trapped atoms, the optical lattices can have an intriguing and rich magnetic structure. The magnetism follows closely the shell structure in the individual lattice wells, emerging as there is an excess of one spin species in a single lattice site. The situation is in fact analogous to the behavior of quantum dot lattices in semiconductors, where the magnetism is governed by the shell structure of the single-dot components[19,20,21].

An optical lattice can be created by counter-propagating laser beams. The resulting potential is a sinusoidal standing wave $V_{opt}(\mathbf{r}) = V_0(\cos^2(kx) + \cos^2(ky))$, where the amplitude V_0 is tuned by laser intensity and the wave number $k = 2\pi/\lambda$ is set by the laser wave length[11]. A natural unit for the energy is the recoil energy $E_R = \hbar^2k^2/(2m)$, and length is measured by the inverse of the wave number. (In experiments, an underlying slowly varying harmonic confinement is added giving rise to an inhomogeneous filling of the lattice and coexistence of insulating and conducting domains. This external confinement can be made small and is neglected here.)

We consider a square lattice with two lattice sites in the unit cell, as sketched in Figure 1(A) and (B). One site resides at the center of the unit cell, and the other one crosses the corner periodically, as indicated in the contour plot of the optical potential. Note that this is the simplest choice of the unit cell allowing for antiferromagnetic alignment of the single-site spins. The inter-site

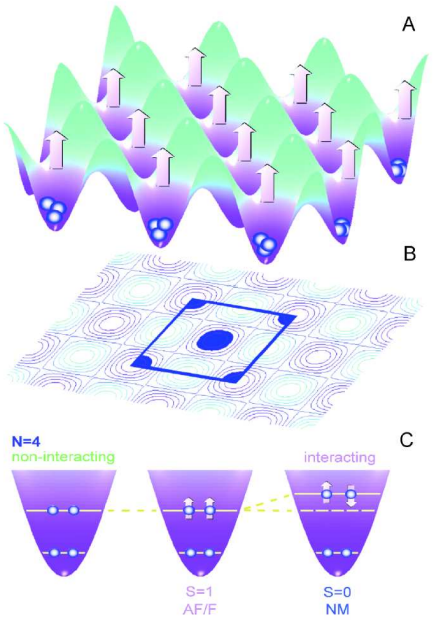

FIG. 1: (A) Schematic sketch of the optical lattice potential, V_{opt}, confining a small number of atoms in each of the potential minima. (Here, the arrows indicate a ferromagnetic ground state as an example). (B) shows the contours of V_{opt} and indicates the unit cell, with one trap at the center of the unit cell, and the second one crossing the corner of the cell periodically. (C) Illustration of Hund's first rule with repulsive contact interactions: the energy is lower as the particles become non-interacting for the same species, i.e. aligned spins (see text).

tunneling can be tuned by varying the lattice depth V_0. With increasing V_0 the atoms become more localized in the lattice sites, the band dispersion decreases and the shells in the individual traps are separated by increasingly large gaps. For sufficiently large lattice depth V_0, it is the shell structure of the the individual atom traps at the lattice sites that determines the physical behavior of the lattice.

The mechanism leading to magnetic effects in the single quantum wells of the lattice is sketched in Figure 1(C). In the two-component contact-interacting fermion gas, due to the Pauli principle there is no mutual interaction between atoms of the same species. Therefore, the trapped atoms in a degenerate shell can lower their interaction energy by maximizing the number of atoms of the same species – in other words, by aligning their spins. This mechanism in contact-interacting atomic systems leads to Hund's first rule[22] and magnetism, in close similarity to long-range interacting electronic systems, as for example, quantum dots in semiconductor heterostructures[23]. Here, however, Hund's rule has a more dramatic effect since it completely removes the interaction between the same atom species.

A Bose-Einstein condensate of a weakly interacting, dilute gas of bosonic atoms is known to be well described by the Gross-Pitaevskii equation for the condensate wave function[24]. Correspondingly, contact-interacting fermions may be approximated by a set of Kohn-Sham-like equations with a local effective potential. We note that in the dilute limit the exchange energy is treated exactly[25]. Periodic boundary conditions imply Bloch form for the orbitals, $\psi_{n\mathbf{k}\sigma}(\mathbf{r}) = \exp(i\mathbf{k}\cdot\mathbf{r})u_{n\mathbf{k}\sigma}(\mathbf{r})$, where n labels the band, $\sigma = (\downarrow,\uparrow)$ is the spin index and the wave vector $\mathbf{k}$ is confined into the first Brillouin zone. The periodic functions $u_{n\mathbf{k}\sigma}(\mathbf{r})$ satisfy

$$-\frac{\hbar^2}{2m}(\nabla + i\mathbf{k})^2 u_{n\mathbf{k}\sigma}(\mathbf{r}) + [V_{opt}(\mathbf{r}) + gn^{\sigma'}(\mathbf{r})]u_{n\mathbf{k}\sigma}(\mathbf{r}) = \varepsilon_{n\mathbf{k}\sigma} u_{n\mathbf{k}\sigma}(\mathbf{r}), \quad \sigma \neq \sigma' \quad (1)$$

where m is the atom mass, n^σ is the density of atom species σ and g is the interaction strength. For the latter we have set $g = 0.3\ E_R/k^2$ in order to stay in the weak-interaction regime, where Eq. 1 is valid. This was confirmed by comparing the mean-field calculations for a single 2D harmonic trap with results obtained by exact diagonalization for $N \leq 8$ (see Y. Yu *et al.,* to be published). For the Bloch wave vector we use a grid of 5×5 points in the first Brillouin zone, and the key results were tested with up to 9×9 points. In the band-structure calculation, the functions $u_{n\mathbf{k}\sigma}(\mathbf{r})$ are expanded in a basis of 11×11 plane waves. The self-consistent iterations were started with antiferromagnetic and ferromagnetic initial potentials and small random perturbations were added to the initial guesses in order to avoid convergence into saddle points of the potential surface.

The results of the calculations in the above scheme are displayed in Figure 2, which shows the systematics of the magnetism as a function of the shell filling of the single quantum wells in the lattice as a function of N and V_0. The calculated points and the different ground state configurations are indicated explicitly in the figure. Filled and open circles are the antiferromagnetic (AF) and ferromagnetic (F) states, respectively. The non-magnetic region at smaller values of V_0 in the phase diagram is shaded and the corresponding states are indicated by squares (NM). The different magnetic phases follow systematically the filling of the single-trap shell structure.

The bottom of the trapping potential can be approximated by a harmonic potential with $\hbar\omega = \sqrt{4V_0 E_R}$. In two dimensions, this leads to the lowest closed shells at particle numbers N =2, 6, and 12 (which are frequently also called "magic numbers" in the literature, refering back to the conventions in nuclear physics)[2]. At higher energies, however, the potential has a notch connecting the different lattice sites which imposes a square symmetry that breaks the three-fold degeneracy of the third, $2s1d$, oscillator shell. Due to this notch, in our case the closed shells correspond to atom numbers N =2, 6, *10* and 12. In these cases, the spins in the single quantum wells are compensated, and the lattice is non-magnetic. However, in between these values, at $N = 1, 4, 8$ and 11, the shells are *half-filled.* Antiferromagnetic ordering of spins is observed as a gap is formed at the Fermi-level. For other atom numbers, the shells are only partially filled, and therefore the Fermi-levels reside in the mid-

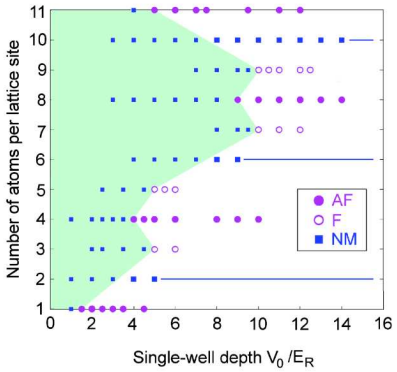

FIG. 2: Magnetism in a square optical lattice, as a function of the lattice depth V_0 (determining the tunneling and coupling between the single wells) in units of the recoil energy E_R, and the particle number (determining the shell filling). The different non-magnetic (NM, *blue squares*), ferromagnetic (F, *empty circles*) and anti-ferromagnetic (AF, *filled circles*) phases are indicated. For closed shells ("magic numbers") at $N = 2, 6$ and 10, the lattice is non-magnetic. The antiferromagnetic ground state is seen at mid-shell only, i.e. at $N = 1, 4$ and 8. In between, i.e. at the beginning and end of a shell, the lattice is ferromagnetic. The shaded area (*green color*) indicates the non-magnetic region at smaller values of V_0.

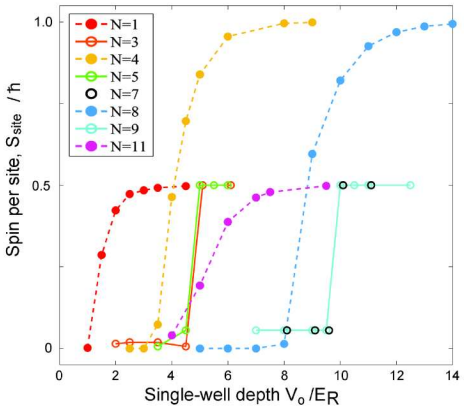

FIG. 3: Integrated spin density over a single lattice site ("spin per site", $S_{\rm site}/\hbar$), as a function of increasing lattice depths V_0 (in units of the recoil energy E_R). The different colors correspond to different particle numbers (shell fillings) of the single traps, as indicated in the inset.

dle of a band. These configurations cannot open a gap. They favor ferromagnetism, as the exchange-like effect splits the spin levels. The lowest band is formed from the $1s$ levels of the individual wells. It can be occupied by at most two atoms per lattice site. By assuming an antiferromagnetic alignment of spins at half-filled band $N = 1$, a gap opens at the Fermi-level since the nearest similar neighbor is twice as far away as in the ferromagnetic lattice where every lattice site is identical. For $N = 3, 4, 5$ and 6 the levels at the $1p$ shell are occupied. At $N = 4$ the spin at the $1p$ shell is maximized due to Hund's first rule. This mid-shell configuration favors antiferromagnetism where the energy is reduced by opening the Fermi-gap. At $N = 3$ the shell has only one atom in a p-shell and at $N = 5$ the shell is nearly filled. In both these cases the Fermi-energy lies on the band and ferromagnetism is found.

At the third shell, $2s1d$, a shell closing at $N = 10$ with a non-magnetic phase, and mid-shell fillings for $N = 8$ and $N = 11$ with antiferromagnetic phases are encountered. This is attributed to the symmetry-breaking of the $2s1d$ shell that resides close to the potential junction between different lattice sites. The d-state whose density lobes are not oriented towards the nearest neighbors is pushed higher in energy. As a result, the $2s1d$ shell is split into two sub-shells, one consisting of $2s$ and $1d$ levels and the other one formed by the higher-lying $1d$ level. Consequently, we find mid-shell fillings at $N = 8$ and 11 leading to antiferromagnetism.

The splitting between the spin bands in the ferromagnetic cases is of the order of 0.050 E_R which correspond to approximately 0.048 k_BT_F in a gas of ^{40}K, where the Fermi-temperature is[26] $T_F = 330\ nK$. The typical energy difference between non-magnetic and ferromagnetic states is 0.001 E_R, corresponding to roughly 0.001 k_BT_F in the fermionic potassium gas. These energies correspond to temperatures which are about a factor of ten lower than the ones achieved experimentally. We mention here that an interaction-induced cooling mechanism was proposed[27] in order to reach the antiferromagnetic phase at $N = 1$.

The onset of magnetism as a function of V_0 can be seen in Figure 3 which shows the "spin per site", obtained by integrating the spin density over a single lattice site,

$$S_{\rm site} = \frac{\hbar}{2}\int_{site}[n^{\uparrow}(\mathbf{r}) - n^{\downarrow}(\mathbf{r})]d\mathbf{r}. \qquad (2)$$

Generally, the magnetism sets on with increasing V_0 as the number of atoms per lattice site becomes larger and, thus, the spatial extent of the highest occupied orbital increases. The transition occurs roughly at the same value of V_0 when the Fermi-level resides at particular shells. For example, the transition occurs at $V_0 \approx 4.2\ E_R$ for atom numbers $N = 3, 4$ and 5 as the $1p$ levels are occupied. For $N = 11$ atoms, antiferromagnetism sets on already around $V_0 = 5\ E_R$. In this case, the highest occupied orbital ($1d$) has only a small overlap with the corresponding orbital at the neighboring site. Therefore, the optical lattice has to be shallow before the tunneling between these levels is large for the magnetism to disappear.

In summary, going beyond the single-band Hubbard model we found that two-component cold fermionic atoms in an optical lattice establish a rich magnetic phase diagram, and can show analogous effects to the electrons in magnetic solids. The magnetism in the optical lattice is determined by the number of atoms per lattice site,

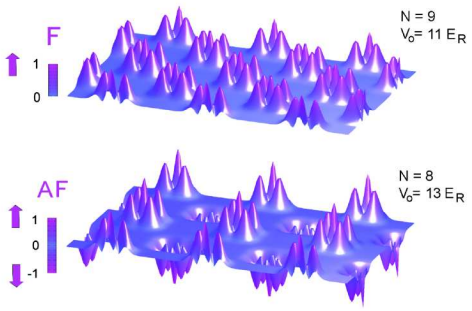

FIG. 4: Spin density $(n_\uparrow - n_\downarrow)$ of the ferromagnetic (F) and antiferromagnetic (AF) states for $N = 9$ ($V_0 = 11E_R$) and $N = 8$ ($V_0 = 13E_R$), respectively. (The amplitude is renormalized to maximum value at unity.)

and the depths of the lattice. If the lattice is shallow, for strong inter-site tunneling the lattice does not show any magnetism. For deeper lattices, where the tunneling is small, the total spin of the N atoms at the single sites is determined by the shell structure in the lattice minima. For closed shells (so-called "magic numbers") at $N = 2, 6, 10$ and 12, the single-wells are non-magnetic. For contact-interacting repulsive fermions, Hund's first rule applies in a particularly dramatic way, removing the interaction between the same atom species. Antiferromagnetic ordering of the single-site spins was found when a gap at the Fermi level could open up. This was the case at mid-shell, with $N = 1, 4, 8$, or 11 particles in the single traps. Ferromagnetism occurred at the beginning and the end of a shell.

[1] Köhl, M. & Esslinger, T. Fermionic atoms in an optical lattice: a new synthetic material. *Europhysics News* **37**, 18 (2006).

[2] Reimann, S. M. & Manninen, M. Electronic structure of quantum dots. *Rev. Mod. Phys.* **74**, 1283 (2002).

[3] Jaksch, D. & Zoller, P. The cold atom Hubbard toolbox. *Annals of Physics* **315**, 52 (2005).

[4] Feshbach, H. Unified Theory of Nuclear Reactions. *Annals of Physics* **5**, 357 (1958).

[5] Inouye, S. Observation of Feshbach resonances in a Bose-Einstein condensate. *et al. Nature* **392**, 151 (1998).

[6] Courteille, Ph. *et al.* Observation of a Feshbach Resonance in Cold Atom Scattering. *Phys. Rev. Lett.* **81**, 69 (1998).

[7] Roberts, J. L. *et al.* Resonant Magnetic Field Control of Elastic Scattering in Cold ^{85}Rb. *Phys. Rev. Lett.* **81**, 5109 (1998).

[8] Duine, R. A. & Stoof, H. T. C. Atom-molecule coherence in Bose gases. *Physics Reports* **396**, 115 (2004)

[9] Theis, M. Tuning the Scattering Length with an Optically Induced Feshbach Resonance. *Phys. Rev. Lett.* **93**, 123001 (2004)

[10] Jaksch, D., Brunder, C., Cirac, J. I., Gardiner, C. W. & Zoller, P. Cold Bosonic Atoms in Optical Lattices. *Phys. Rev. Lett.* **81**, 3108 (1998).

[11] Greiner, M., Mandel, O., Esslinger, T., Hänsch, T. W. & Bloch, I. Quantum phase transition from a superfluid to a Mott insulator in a gas of ultracold atoms. *Nature* **415**, 39 (2002).

[12] Stöferle, T., Moritz, H., Schori, C., Köhl, M. & Esslinger, T. Transition from a Strongly Interacting 1D Superfluid to a Mott Insulator. *Phys. Rev. Lett.* **92**, 130403 (2004).

[13] Xu, K. Sodium Bose-Einstein condensates in an optical lattice. *Phys. Rev.* A **72**, 043604 (2005).

[14] Köhl, M., Moritz, H., Stöferle, T., Günter, K., and Esslinger, T. Fermionic Atoms in a Three Dimensional Optical Lattice: Observing Fermi Surfaces, Dynamics, and Interactions. *Phys. Rev. Lett.* **94**, 080403 (2005)

[15] Köhl, M., Günter, K., Stöferle, T., Moritz, H. & Esslinger, T. Strongly Interacting Atoms and Molecules in a 3D Optical Lattice. http://arxiv.org/abs/cond-mat/0605099 (2006)

[16] Drummond, P. D., Corney, J. F., Liu, X.-J. & Hu, H. Ultra-cold fermions in optical lattices. *Journal of Modern Optics* **52** No. 16, 2261-2268 (2005).

[17] Vollhardt, D. in Broglia, R. A., Schrieffer, J. R. & Bortignon, P. F. (editors) *Perspectives in Many-Body Physics.* North-Holland, Amsterdam, (1994)

[18] Honerkamp, C., & Hofstetter, W., Ultracold Fermions and the SU(N) Hubbard Model. *Phys. Rev. Lett.* **92**, 170403 (2004).

[19] Koskinen, M., Reimann, S. M., & Manninen M. Spontaneous Magnetism of Quantum Dot Lattices. *Phys. Rev. Lett.* **90**, 066802 (2003).

[20] Koskinen, P., Sapienza, L. & Manninen, M. Tight-Binding Model for Spontaneous Magnetism of Quantum Dot Lattices. *Physica Scripta* **68**, 74 (2003).

[21] Kolehmainen, J., Reimann, S. M., Koskinen, M. & Manninen, M. Magnetic interaction between coupled quantum dots *Eur. Phys. J. B* **13**, 731 (2000).

[22] Weissbluth, M. *Atoms and Molecules.* Academic Press, N.Y., (1978).

[23] Koskinen, M., Manninen, M. & Reimann, S. M. Hund's Rules and Spin Density Waves in Quantum Dots. *Phys. Rev. Lett.* **79**, 1389 (1997).

[24] Dalfovo, F., Giorgini, S., Pitaevskii, L. P. & Stringari, S. Theory of Bose-Einstein condensation in trapped gases. *Rev. Mod. Phys.* **71**, 463 (1999).

[25] Magyar, R. J. & Burke, K. Density-functional theory in one dimension for contact-interacting fermions. *Phys. Rev. A* **70**, 032508 (2004).

[26] Pezzè, L. *et al.* Insulating Behavior of a Trapped Ideal Fermi Gas. *Phys. Rev. Lett.* **93**, 120401 (2004).

[27] Werner, F. , Parcollet, O., Georges, A. & Hassan, S. R. Interaction-Induced Adiabatic Cooling and Antiferromagnetism of Cold Fermions in Optical Lattices. *Phys. Rev. Lett.* **95**, 056401 (2005).

Acknowledgement: This work was financially supported by the Swedish Research Council, the Swedish Foundation for Strategic Research, the Finnish Academy of Science, and the European Community project ULTRA-1D (NMP4-CT-2003-505457).

Correspondence should be adressed to S.M. Reimann, stephanie.reimann@matfys.lth.se